Computers in Biology and Medicine 100 (2018) 270–278

Contents lists available at ScienceDirect

Computers in Biology and Medicine

journal homepage: www.elsevier.com/locate/compbiomed

Deep convolutional neural network for the automated detection and diagnosis of seizure using EEG signals

U. Rajendra Acharya [a,b,c,*], Shu Lih Oh [a], Yuki Hagiwara [a], Jen Hong Tan [a], Hojjat Adeli [d]

[a] Department of Electronics and Computer Engineering, Ngee Ann Polytechnic, Singapore
[b] Department of Biomedical Engineering, School of Science and Technology, SUSS University, Singapore
[c] Department of Biomedical Engineering, Faculty of Engineering, University of Malaya, Malaysia
[d] Departments of Neuroscience, Neurology, Biomedical Engineering, Biomedical Informatics, and Civil, Environmental, and Geodetic Engineering, The Ohio State University, 470 Hitchcock Hall, 2070 Neil Avenue, Columbus, OH, 43210, United States

ARTICLE INFO

Keywords:
Epilepsy
Convolutional neural network
Encephalogram signals
Deep learning
Seizure

ABSTRACT

An encephalogram (EEG) is a commonly used ancillary test to aide in the diagnosis of epilepsy. The EEG signal contains information about the electrical activity of the brain. Traditionally, neurologists employ direct visual inspection to identify epileptiform abnormalities. This technique can be time-consuming, limited by technical artifact, provides variable results secondary to reader expertise level, and is limited in identifying abnormalities. Therefore, it is essential to develop a computer-aided diagnosis (CAD) system to automatically distinguish the class of these EEG signals using machine learning techniques. This is the first study to employ the convolutional neural network (CNN) for analysis of EEG signals. In this work, a 13-layer deep convolutional neural network (CNN) algorithm is implemented to detect normal, preictal, and seizure classes. The proposed technique achieved an accuracy, specificity, and sensitivity of 88.67%, 90.00% and 95.00%, respectively.

1. Introduction

According to the World Health Organization (WHO), nearly 50 million people suffer from epilepsy worldwide [1]. It is estimated that 2.4 million people are diagnosed with epilepsy annually [1].

Seizures are due to the uncontrolled electrical discharges in a group of neurons [2,3]. The excessive electrical discharges result in the disruption of brain function. Epilepsy is diagnosed when there is recurrence of at least two unprovoked seizures. It can affect anyone at any age [4].

A timely and accurate diagnosis of epilepsy is essential for patients in order to initiate anti-epileptic drug therapy and subsequently reduce the risk of future seizures and seizure-related complications [5]. Currently, the diagnosis of epilepsy is made by obtaining a detailed history, performing a neurological exam, and ancillary testing such as neuro-imaging and EEG. The EEG signals can identify inter-ictal (between seizures) and ictal (during seizure) epileptiform abnormalities.

Fig. 1 shows a graphical representation of the electrical activity in the brain of healthy subjects and seizure patients. Typically, neurons communicate through electrical signals. Therefore, in a regular brain activity, these electrical signals are normally regulated [3] (see the normal activity in Fig. 1). However, during seizure, there is an abnormally increased hyper-synchronous electrical activity of epileptogenic neural network. This activity may remain localized to one part of the brain, or spread to the entire brain. In either scenario, an individual may experience a clinical seizure (see the seizure activity in Fig. 1) [3]. Neurologists scrutinize the EEG via direct visual inspection to investigate for epileptiform abnormalities that may provide valuable information on the type and etiology of a patient's epilepsy.

However, interpretation of the EEG signals by visual assessment is time-consuming particularly with the increased use of out-patient ambulatory EEG's and in-patient continuous video EEG recordings, where there are hours or days worth of EEG data that needs to be reviewed manually [6]. The majority of EEG software includes some form of automated seizure-detection, however, due to the poor sensitivity and specificity of the pre-determined seizure detection algorithms, the current forms of automated seizure detection are rarely used in clinical practice. In addition, the inherent nature of visual inspection results in varying clinical interpretations based on the EEG reader's level of expertise in electroencephalography. Complicating matters, the quality of the study may be confounded by interfering artifactual signal limiting the reader's ability to accurately identify abnormalities. Moreover, the low yield of routine out-patient studies poses another problem. A patient

* Corresponding author. Department of Electronics and Computer Engineering, Ngee Ann Polytechnic, 599489, Singapore.
E-mail address: aru@np.edu.sg (U.R. Acharya).

https://doi.org/10.1016/j.compbiomed.2017.09.017
Received 27 July 2017; Received in revised form 29 August 2017; Accepted 22 September 2017

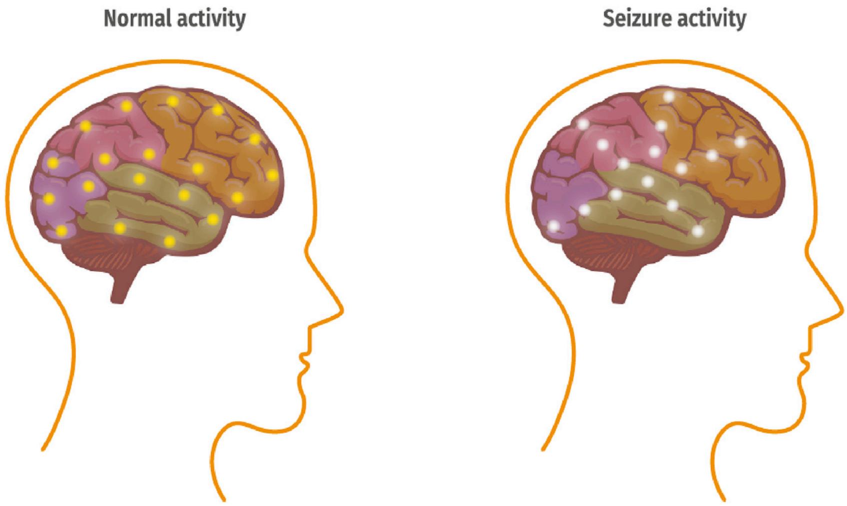

Fig. 1. An illustration of normal and seizure activity in the brain.

with epilepsy can go for an outpatient EEG and the study may be completely normal. This is because the brains of patients with epilepsy are generally not continually firing off epileptic discharges. An EEG is simply a "snapshot" of their brain at the moment of recording. The sensitivity of identifying epileptic discharges can be increased by having the patient come back for repeated outpatient studies or recording them for longer periods of time, either via a home ambulatory study or an inpatient continuous video EEG monitoring study, which are both costly and time-intensive for the patient and for the physician reading the EEG.

Patients are referred to an epilepsy monitoring unit for inpatient continuous video EEG monitoring for a couple different reasons. Usually it is done when the diagnosis of epilepsy is not clear, i.e., a patient's history is atypical for a seizure disorder or could represent another condition clinically similar to seizure, i.e. syncope, or if there is no improvement in seizure frequency following anti-epileptic drug administration. The patient is admitted to the hospital and hooked up to an EEG for several days. If they are on anti-epileptic medications, they are discontinued. The whole point is for them to have their seizure or seizure-like event while they are hooked up to the EEG machine. Then, a trained neurologist or epileptologist analyzes the clinical characteristics of the event in conjunction with visual inspection of the EEG to determine if the patient has epilepsy or not. The increased amount of data also allows the epileptologist to look for inter-ictal abnormalities. Generally, during a seizure, the EEG activity becomes very abnormal and can be clearly determined whether the patient's events are epileptic or non-epileptic. The epileptic EEG signals are more chaotic and varies more as compared to the normal EEG signals. During seizure, there is a sudden surge in neural discharge resulting in the increase of disparities in EEG signals. The neurons in the cerebral hemispheres during a seizure misfire and produce abnormal electrical activity. Thus, the number of neurons available for data processing during seizures decreases. However, at times this can be very difficult because some patients with epilepsy, usually patients with frontal lobe epilepsy or seizures emanating from a deep source or a very small area, can have a clinical seizure and the ictal EEG is normal. Although epileptiform abnormalities are invariably present, these abnormalities do not register on scalp surface electrodes. This can therefore make the diagnosis very difficult. In patients with intractable epilepsy undergoing surgical evaluation, invasive intracranial depth electrodes and/or grids are utilized to identify the epileptogenic zone, which carries peri-procedural risks and complications.

Fig. 2 displays sample normal, interictal, and seizure EEG signals from the Bonn University database. The visual interpretation of these signals is prone to inter-observer variabilities. Therefore, for an accurate, fast, and objective diagnosis a computer-aided diagnosis (CAD) system is advocated. Since the seminal article by Adeli et al. [7], automated EEG-based seizure detection and epilepsy diagnosis has been the subject of significant research. Many researchers have proposed different approaches to automatically detect epileptic seizure using EEG signals. For reviews of this literature, see Acharya et al. [8] and Faust et al. [9] where different approaches, namely, time, frequency, time-frequency, and nonlinear methods are discussed. Acharya et al. [10] also review application of entropies for automated EEG-based diagnosis of epilepsy.

The EEG signal is nonlinear and nonstationary in nature thus; the signal is highly complex and is difficult to visually interpret the signals (see Fig. 2). Based on the reviews [8–10], it can be observed that the researchers have extracted features, performed statistical analysis, ranked the features, and classified the best classifier by comparing the performance of different classifiers. Thus, the workflow consists of many

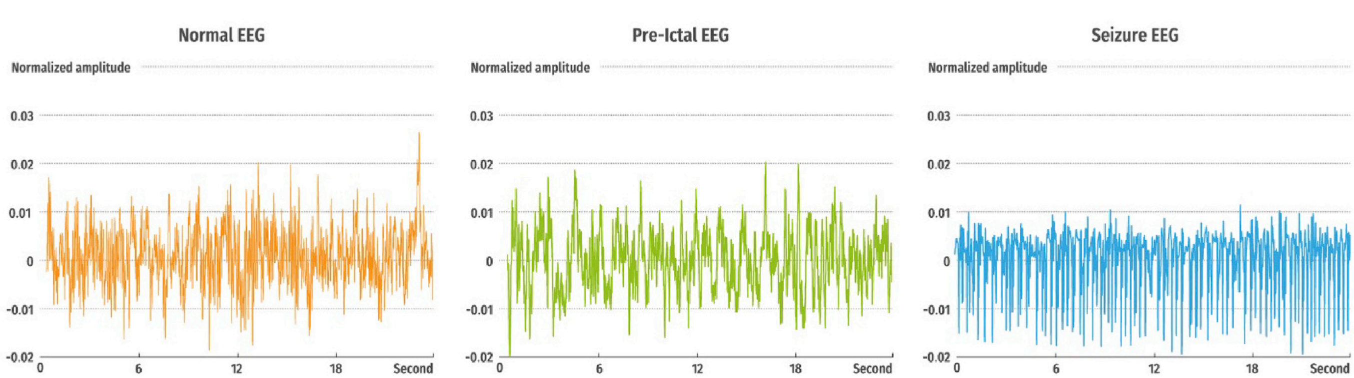

Fig. 2. Sample normal, preictal, and seizure EEG signals from the Bonn University database.

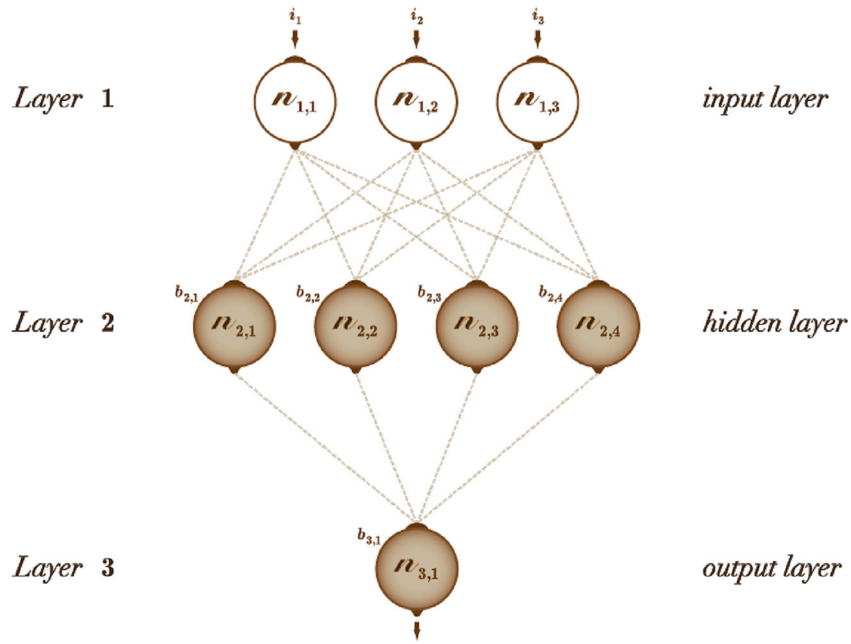

Fig. 3. An illustration of a typical structure of ANN.

standard steps. This work proposes implementation of deep learning for an automated detection of normal, preictal, and seizure EEG signals without performing feature extraction and selection.

Deep learning is a machine learning technique based on representation learning where the system automatically learns and discovers the features needed for classification from the processing of multiple layers of input data [11]. Deep learning has already proven its capability and has outperformed humans in audio and image recognition tasks [11,12]. It has been used in many other diverse complicated machine learning applications such as early diagnosis of the Alzheimer's disease [13], prediction of sale prices of real estate units [14], estimation of concrete compressive strength [15]. Moreover, many large technology companies such as Apple, Baidu, Google, IBM, Facebook, Microsoft, and Netflix have embraced and utilized deep learning in their research [16–18]. In this study, a deep learning method is employed to automatically identify the three classes of EEG signals. To the best the authors' knowledge, this is the first EEG study to employ deep learning algorithm for the automated classification of three EEG classes. A 13-layer deep convolutional neural network (CNN) is developed to categorize the normal, preictal, and seizure class.

2. Data

EEG segments used in this research are those collected by Andrzejak et al. [19] at Bonn University, Germany (http://epilepsy.uni-freiburg.de/database). The segments were selected from continuous multichannel EEG recordings with artifacts removed via visual examination due to muscle activity and eye movements.

The dataset obtained from 5 patients contains three classes of data, namely, normal (Set B), preictal (Set D), and seizure (Set E). There is a total of 100 EEG signals in each dataset. Each record is a single channel EEG signal with a duration of 23.6 s. The normal dataset comprises of EEG signals obtained from 5 healthy subjects, each containing 100 cases. Similarly, the preictal class contains 100 data from 5 epileptic patients, when they did not undergo seizure during the time of acquisition. The seizure class consists of 100 cases with the same subjects when they were having epilepsy during the time of signals acquisition.

3. Methodology

3.1. Pre-processing

Each EEG signal is normalized with Z-score normalization, zero mean and standard deviation of 1 before feeding into the 1-D deep convolutional network (CNN) for training and testing. The sampling rate of the EEG signal is set at 173.61 Hz.

3.2. Artificial neural network (ANN)

Generally, an ANN has *three* layers: input, hidden, and output layers (see Fig. 3) [20]. The concept of ANN is inspired by complex networks structure found in human brains. ANN is made up of a collection of connected units called nodes or neurons. Just like the biological neuron found in the brain, these neurons integrate the input signals and transmit them to other connected neurons. The output of the neurons is subjected to the weighted sum given by the previous layer of neurons. However, the ANN model is susceptible to shift and translation distortion which may result in poor classification accuracy [21].

3.3. Convolutional neural network (CNN)

An improved and recently-developed neural network, known as Convolutional Neural Network (CNN) is employed in this research. The improved ANN is both shift and translational invariance [21]. The convolution operation in.

CNN is a subset of deep learning which has attracted a lot of attention in recent year and used in image recognition such as analysis of x-ray medical images [22], magnetic resonance images [23], histopathological images [24], fundus images [25], and computed tomography images [26]. But, very little research has been done on the use of CNN using physiological signals. Thus, in the authors' previous works [27–30], CNN was implemented on ECG signals to study the effectiveness of the CNN algorithm in analysis of signals. The CNN was employed to automatically detect arrhythmias using different intervals of tachycardia ECG segments with accuracies of 92.5% and 94.9% using 2-s and 5-s ECG segments, respectively [28]. CNN was recently employed in the automated

Table 1
The details of CNN structure used in this research.

Layers	Type	Number of neurons (output layer)	Kernel size for each output feature map	Stride
0–1	Convolution	4092 × 4	6	1
1–2	Max-pooling	2046 × 4	2	2
2–3	Convolution	2042 × 4	5	1
3–4	Max-pooling	1021 × 4	2	2
4–5	Convolution	1018 × 10	4	1
5–6	Max-pooling	509 × 10	2	2
6–7	Convolution	506 × 10	4	1
7–8	Max-pooling	253 × 10	2	2
8–9	Convolution	250 × 15	4	1
9–10	Max-pooling	125 × 15	2	2
10–11	Fully-connected	50	–	–
11–12	Fully-connected	20	–	–
12–13	Fully-connected	3	–	–

diagnosis of myocardial infraction [27] and coronary artery disease [29]. Furthermore, the authors classified different classes of heartbeats [30] using ECG signals.

Similar to the ANN, the final output decision of the CNN model is based on the weights and biases of the previous layers in the network structure. Hence, the weights and biases of the model are updated with Equation (1) and Equation (2) respectively for each layer.

$$\Delta W_l(t+1) = -\frac{x\lambda}{r}W_l - \frac{x}{n}\frac{\partial C}{\partial W_l} + m\Delta W_l(t) \tag{1}$$

$$\Delta B_l(t+1) = -\frac{x}{n}\frac{\partial C}{\partial B_l} + m\Delta B_l(t) \tag{2}$$

where *W, B, l, λ, x, n, m, t,* and *C* represent the weight, bias, layer number, regularization parameter, learning rate, total number of training samples, momentum, updating step, and cost function respectively.

The parameters used to train the CNN model are (i) lambda (regularization), (ii) learning rate, and (iii) momentum. These parameters can be tuned according to the dataset in order to achieve optimum performance [6]. The lambda is to prevent overfitting of the data. The learning rate is to control how fast the network learns during training and momentum helps to convergence the data. The parameters lambda, learning rate, momentum is set to 0.7, 1×10^{-3}, and 0.3 respectively in this work. These parameters are obtained by trial-and error.

To the best of the authors' knowledge, this research is the first implementation of CNN for EEG signal processing in general and seizure detection in particular.

The CNN architecture consists of three different types of layer: (1) convolutional layer, (2) pooling layer, and (3) a fully connected layer [17].

(1) **Convolutional layer**: It consists of filters (kernels) which slide across the EEG signal. A kernel is the matrix to be convolved with the input EEG signal and stride controls how much the filter convolves across the input signal. This layer performs the convolution on the input EEG signals with the kernel using Equation (3). The output of the convolution is also known as the feature map.

The convolution operation is as follows:

$$y_k = \sum_{n=0}^{N-1} x_n h_{k-n} \tag{3}$$

where x is signal, h is filter, and N is the number of elements in x. The output vector is y. The subscripts denote the nth element of the vector.

(2) **Pooling layer**: This layer is also known as the down-sampling layer. The pooling operation reduces the dimension of output neurons from the convolutional layer to reduce the computational intensity and prevent the overfitting. The max-pooling operation is used in this work. Max-pooling operation selects only the maximum value in each feature map and consequently reducing the number of output neurons.
(3) **Fully connected layer**: This layer has full connection to all the activations in the previous layer.

Two types of activation functions are used in this work: (1) Rectified linear activation unit and (2) softmax.

(1) **Rectified linear activation unit**: After every convolutional layer, it is a common practice to employ an activation function. Activation function is an operation which maps an output to a set of inputs. They are used to impart non-linearity to the network structure. The rectifier linear unit is an established activation function for deep learning [17]. The leaky rectifier linear unit [31] (LeakyRelu) is used in this work as an activation function for the convolutional layers (1, 3, 5, 7, 9, 11, and 12). LeakyRelu has properties which adds nonlinearity and sparsity in the network structure. Therefore, providing robustness to small changes such as noise in the input. Equation (4) shows the LeakyRelu function.

$$f(x) = \begin{cases} x & \text{if } x > 0 \\ 0.01x & \text{otherwise} \end{cases} \tag{4}$$

(2) **Softmax**: This function computes the probability distribution of the k output classes. Hence, Layer 13 uses softmax function to predict which class the input EEG signal (normal, preictal, or seizure) belongs to.

$$p_j = \frac{e^{x_j}}{\sum_1^k e^{x_k}} \quad \text{for } j = 1, \ldots k$$

where x is the net input. Output values of p are between 0 and 1 and their sum equals to 1.

3.4. Architecture

Table 1 is the summary of details of the proposed CNN structure. The parameters (kernel size) in Table 1 are derived through trial-and-error. Fig. 4 shows the graphical representation of CNN structure with 4097 input sample lengths where the green, blue, and red color signify the kernel size, max-pooling, and fully connected layer respectively. This proposed CNN architecture includes five convolutional, five max-pooling, and three fully connected layers (total of eleven layers deep CNN). The stride is set at 1 and 2 for convolution of the EEG signals and max-pooling operations respectively.

The input layer (Layer 0 in Fig. 4) is convolved using Equation (3) with a kernel of size 6 to produce Layer 1. Then, a max-pooling of size 2 is applied to every feature map (Layer 2). After the max-pooling operation, the number of neurons is reduced from 4092 × 4 to 2046 × 4. Again, the feature map in Layer 2 is convolved with a kernel of size 5 to produce Layer 3. A max-pooling operation of size 2 is applied to every feature map (Layer 4), reducing the number of neurons to 1021 × 4. Then, feature map from Layer 4 is convolved with a kernel of size 4 to produce Layer 5. Again, a max-pooling of size 2 is applied to reduce the number of neurons in the output layer to 509 × 10 (Layer 6). The feature map in Layer 6 is again convolved with a kernel size of 4 to produce the next layer (Layer

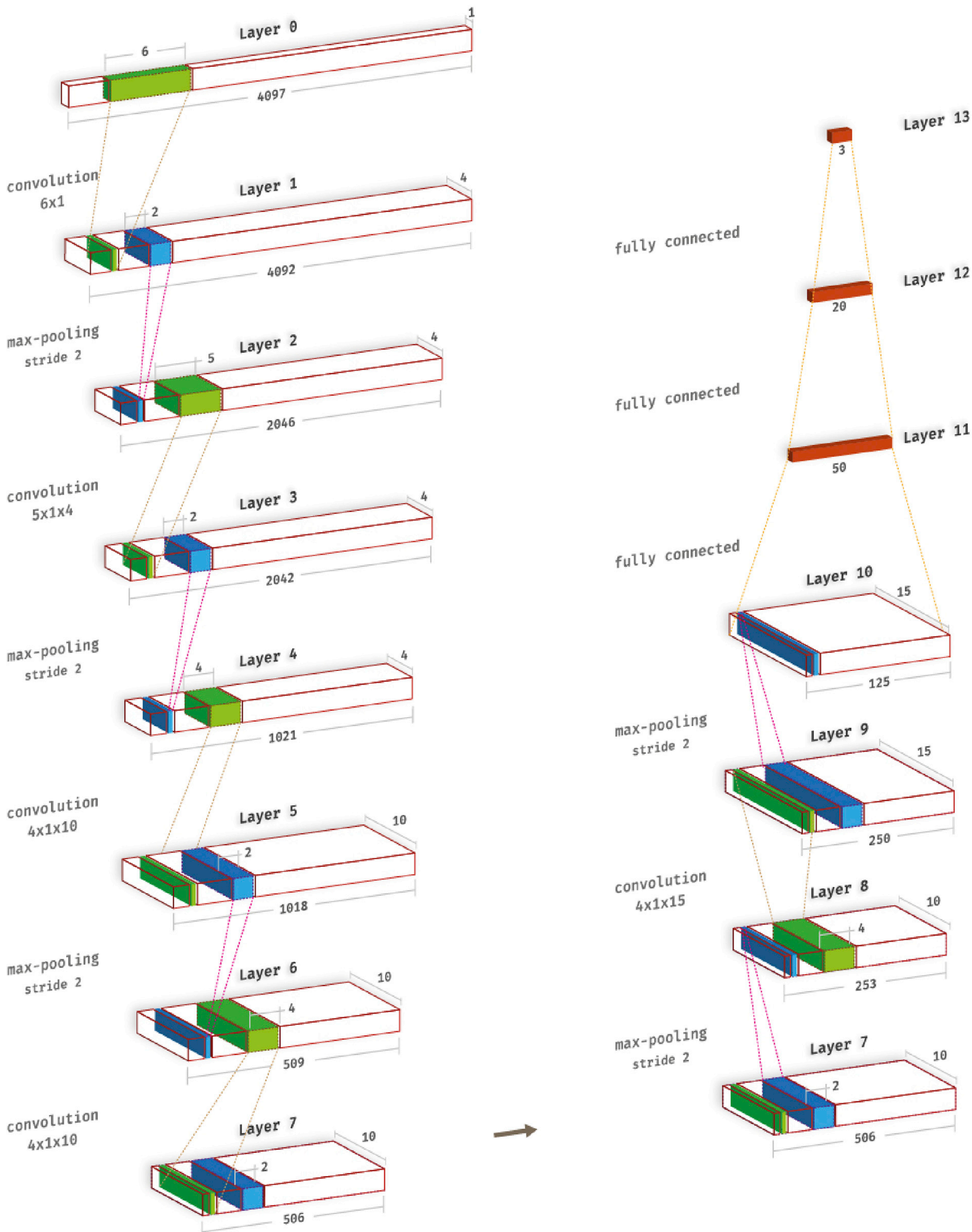

Fig. 4. The proposed net structure implemented in this work.

7). Likewise, a max-pooling of size 2 is applied to the feature map (Layer 8). The feature map in Layer 8 is convolved with a kernel of size 4 to produce Layer 9. Once more, a max-pooling of size 2 is applied to every feature map in Layer 10. Eventually, in Layer 10, the neurons are fully connected to 50 neurons in Layer 11 and Layer 11 is fully connected to 20 neurons in Layer 12. Finally, Layer 12 is connected to the last layer (Layer 13) with *3* output neurons (representing normal, preictal, and seizure classes).

3.5. Training of CNN

A conventional backpropagation (BP) [32] with a batch size of 3 is employed in this work to train CNN. BP is a method to calculate the gradient of the loss function with respect to the weights. BP passes error

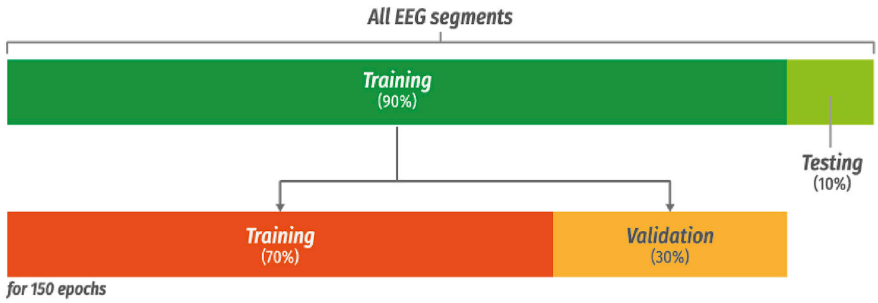

Fig. 5. The allocation of EEG data used for training and testing the proposed algorithm.

Table 2
The confusion matrix across all ten-folds.

		Predicted			Accuracy (%)	PPV (%)	Sensitivity (%)	Specificity (%)
		Normal	Preictal	Seizure				
Original	Normal	90	1	9	93.33	90.00	90.00	95.00
	Preictal	4	88	8	93.67	92.63	88.00	96.50
	Seizure	6	6	88	90.33	83.81	88.00	91.50

Table 3
The overall classification result across all ten-folds.

tp	*tn*	*fp*	*fn*	Accuracy (%)	PPV (%)	Sensitivity (%)	Specificity (%)
190	90	10	10	88.67	95.00	95.00	90.00

*tp = true positive, tn = true negative, fp = false positive, fn = false negative.

signals backwards through the network during training in order for the weights to get updated to the network. A batch size is the number of signals used for each training update. The batch size of 3 is chosen in this work.

3.6. Testing of CNN model

A total of 150 epochs of training were run in this work. An epoch refers to one iteration of the full training set. After every iteration of an epoch, our algorithm validates the CNN model by using 30% of the total training dataset (90%) to validate the model. This is to prevent overfitting of the CNN model during training. Fig. 5 shows the distribution of all the EEG signals used in this work.

3.6.1. k-fold cross-validation

A *ten*-fold cross-validation [33] approach was used in this study. First, the EEG signals are randomly divided into ten equal portions. Nine out of ten portions of EEG signals are used to train the CNN while the remaining one-tenth of the EEG signals are used to test the performance of the system. This strategy is repeated ten times by shifting the test and training dataset. The accuracy, sensitivity, and specificity values reported in the paper are the average values obtained from ten evaluations.

4. Results

The proposed algorithm was implemented on a workstation with two Intel Xeon 2.40 GHz (E5620) processor and a 24 GB random-access memory (RAM) using the MATLAB programming software. It typically took about 12.8 s to complete an epoch of training.

The tabulated confusion matrix across all ten-folds is presented in Table 2. It is observed that 90% of the normal EEG signals are correctly classified as normal EEG signals. Further, a small percentage of 1% and 9% of the normal EEG signals are wrongly classified as preictal and seizure, respectively. Moreover, a high percentage of 88% of EEG signals are correctly classified as preictal signals with 12% of the EEG signals wrongly classified as normal (4%) and seizure (8%) classes. Similarly, 88% of the EEG signals are correctly classified as seizure class with 12% wrongly classified as normal (6%) and preictal (6%) classes.

The performance (specificity, sensitivity, and accuracy) of the proposed model is summarized in Table 3.

5. Discussion

Table 4 presents a summary of studies conducted in the automated detection of normal, preictal, and seizure EEG signals obtained from the Bonn University database.

Adeli et al. [34] presented a wavelet-chaos approach to analyze 6-s EEGs and the different subbands (delta, theta, alpha, beta, and gamma) of EEGs for the identification of seizure and epilepsy through integration of wavelets [35], a signal processing technique, and chaos theory from nonlinear science [36]. Chaos theory is employed as a mathematical microscope to glean into brain waves presented by EEG signals. The nonlinear nature of the EEG signals is characterized using the correlation dimension and the largest Lyapunov exponent to represent the system complexity and system chaoticity respectively. Ghosh-Dastidar et al. [37] introduce a mixed-band wavelet-chaos-neural network (NN) methodology for epilepsy diagnosis as well as epileptic seizure detection. They discovered a 9-parameter mixed-band feature space yielding an accuracy of 96.7% with the Levenberg-Marquardt backpropagation neural network. Ghosh-Dastidar et al. [38] propose a principal component analysis-enhance classifier for robust and reliable categorization of EEG signals into ictal, interictal, and healthy categories. This research resulted in a classification accuracy of 99.3%.

In the past two decades, pulse encoding-based neurons, called spiking neurons, have been proposed that incorporate the temporal aspect of neuronal firing [39]. Using spiking neurons, a new generation of neural networks has been developed, called Spiking Neural Networks (SNN) [40–42]. Ghosh-Dastidar and [43] present an improved SNN model with applications for epilepsy and epileptic seizure detection. They report a classification accuracy of 92.5%. Ghosh-Dastidar and Adeli [40] present a multi-spiking neural network where information from one neuron to the next is transmitted in the form of multiple spikes via multiple synapses along with a new supervised learning algorithm. The model and learning algorithm have been applied to the 3-class EEG classification problem with a classifier accuracy in the range of 90.7%–94.8%.

Acharya et al. [44–50] have developed several CAD algorithms to characterize normal, preictal, and seizure EEG signals. They employed discrete wavelet transform (DWT) [48,50], entropy [46,49], higher

Table 4
A comparison of selected studies in the automated detection of Normal, Preictal, and Seizure classes using EEG signals using the Bonn University database.

Author (Year)	Novelty of paper	Classifier	Performance (accuracy in %)
Ghosh-Dastidar and Adeli (2007) [43]	• Spike neural network learning algorithms.	Spiking neural network	ACC: 92.5%
Ghosh-Dastidar et al. (2007) [41]	• Wavelet chaos methodology. • Nonlinear features.	Levenberg-Marquardt backpropagation neural network	ACC: 96.7%
Ghosh-Dastidar et al. (2008) [37]	• Wavelet chaos methodology.	Principal component analysis enhanced cosine radial basis function neural network	ACC: 99.3%
Ghosh-Dastidar et al. (2009) [60]	• Multi-spike prop.	Multi-spiking neural network	ACC: 90.7%–94.8%
Acharya et al. (2009) [44]	• Nonlinear features.	GMM	SEN: 92.2% SPEC: 100%
Chua et al. (2009) [51]	• HOS feature.	GMM	ACC: 93.1% SEN: 97.7% SPEC: 92%
Chua et al. (2010) [52]	• HOS based entropy features.	GMM	ACC: 93.1% SEN: 89.7% SPEC: 94.8%
Faust et al. (2010) [53]	• Power spectral density estimation methods.	SVM	ACC: 93.3% SEN: 98.3% SPEC: 96.7%
Acharya et al. (2011a) [49]	• Discrete wavelet transform. • Higher cumulant features.	SVM	ACC: 96.3% SEN: 100% SPEC: 97.9%
Acharya et al. (2011b) [47]	• Recurrence quantification analysis.	SVM	ACC: 95.6% SEN: 98.9% SPEC: 97.8%
Guo et al. (2011) [55]	• Genetic programming.	KNN	ACC: 93.5%
Acharya et al. (2012a) [46]	• Entropy, Higher order spectra, nonlinear features.	Fuzzy sugeno	ACC: 99.7% SEN: 100% SPEC: 100%
Acharya et al. (2012b) [45]	• Entropy.	Fuzzy sugeno	ACC: 98.1% SEN: 99.4% SPEC: 100%
Acharya et al. (2012c) [48]	• Wavelet packet decomposition.	Fuzzy sugeno	ACC: 96.7% SEN: 95% SPEC: 99%
Acharya et al. (2012d) [50]	• Discrete wavelet transform.	SVM	ACC: 96% SEN: 96% SPEC: 97%
Martis et al. (2012) [59]	• Empirical mode decomposition. • Hilbert transform.	C4.5 decision tree	ACC: 95.3% SEN: 98% SPEC: 97%
Bhattavharyya et al. (2017a) [61]	• Empirical mode decomposition.	Random forest	ACC: 99.4% SEN: 97.9% SPEC: 99.5%
Bhattavharyya et al. (2017b) [62]	• Tunable Q-wavelet transform.	SVM	ACC: 98.6%
Sharma et al. (2017) [63]	• Analytic time-frequency flexible wavelet transform. • Fractal dimension.	LS-SVM	SEN: 100%
This work	• **Ten-fold cross validation strategy.** • **13-layer deep CNN structure.**	**Convolutional neural network**	**ACC: 88.7%** **SEN: 95%** **SPEC: 90%**

*ACC: accuracy, SEN: sensitivity, SPEC: specificity.
The bold texts represent the proposed work.

cumulant [49], higher order spectra (HOS) [46], nonlinear [44,46,47], and wavelet packet decomposition [48] feature extraction techniques to extract useful information from the EEG signals. Further, it is reported in Acharya et al. [46] that feeding entropy, HOS, and nonlinear features into fuzzy sugeno classifier achieved an accuracy of 99.7% and a sensitivity and specificity of 100%.

Chua et al. [51] extracted higher order spectra (HOS) features to differentiate the three different classes (normal, interictal, ictal). They employed a Gaussian mixture model (GMM) classifier and achieved 93.1% accuracy. In their later study, they improved by combining HOS and entropy features with GMM classifier. They obtained an accuracy, sensitivity, and specificity of 93.1%, 89.7%, and 94.8% respectively [52]. Faust et al. [53], compared the effectiveness of three different model-based spectral density estimation methods namely Yule-Walker, Burg's, and the autoregressive moving average techniques for the characterization of the EEG signals. They reported that Burg's approach with support vector machine (SVM) classifier [54] yielded 93.3% accuracy, 98.3% and 96.7% sensitivity and specificity respectively. Guo et al. [55], employed genetic programming to automatically extract useful features from the EEG signals. Their method self-learns and automated the feature selection process. They reported an accuracy of 93.5% with the k-nearest neighbor classifier. Zhang and Zhou [56] discuss multifractal analysis for seizure detection in intracranial EEG using SVM. Vahabi et al. [57] online epileptic seizure prediction using wavelet-based bi-phase correlation of electrical signal tomography. Yuan et al. [58] describe epileptic seizure detection using the Log-Euclidean Gaussian kernel-based sparse representation. Martis et al. [59] proposed a combination of empirical mode decomposition and Hilbert transform approaches to detect the three EEG classes. They achieved an accuracy of 95.3%.

In this work, the main novelty is the implementation of a deep CNN model for the automated classification of EEG signals into normal, preictal, and seizure classes. A 13-layer CNN is proposed as it provides good convergence and the highest performance accuracy. All parameters of the CNN structure are carefully fine-tuned in order to obtain a model with optimal convergence rate. Deep network allows more complex, nonlinear function to be learned, however such network can be difficult to converge. On the other hand, shallow network is easier to train but the feature extracted are simple and may not be adequate for classification.

Even though this proposed model could not yield the best classification performance as compared to the published works recorded in Table 4, the proposed CNN model still managed to obtain 88.67% accuracy, 95.00% sensitivity, and 90.00% specificity. This shows that given more EEG data, the proposed model can achieve better results with minimum pre-processing of the EEG data. Thus, the overall diagnostic performance using the proposed model can be improved with more numbers of EEG data.

6. Conclusion

A novelty of this proposed model is being the first application of deep neural network for EEG-based seizure detection. A *13*-layer deep learning CNN algorithm is implemented for the automated EEG analysis. An average accuracy of 88.7% is obtained with a specificity of 90% and a sensitivity of 95%. The performance (accuracy, sensitivity, and specificity) of proposed model is slightly lower than some of the works summarized in Table 4. The advantage of the model presented in this paper, however, is separate steps of feature extraction and feature selection are not required in this work. Nevertheless, the main drawback of this work is the lack of huge EEG database. Proposed algorithm requires a diversity of data to obtain an optimum performance. The performance of this technique can be improved by applying a bagging algorithm and increasing the number of samples.

Conflict of interest

There is no conflict of interest in this work.

Acknowledgements

Authors thank Dr. Amir Adeli, Board-Certified Neurologist, Columbus, Ohio, for reviewing the manuscript several times from the perspective of neurologist and providing valuable clinical inputs which improved the paper considerably.

References

[1] World Health Organization, Epilepsy, 2017. http://www.who.int/mediacentre/factsheets/fs999/en/.
[2] American Epilepsy Society, Facts and Figures. https://www.aesnet.org/for_patients/facts_figures.
[3] Harvard Health Publications, Harvard Medical School, Seizure Overview, 2014. http://www.health.harvard.edu/mind-and-mood/seizure-overview.
[4] International League Against Epilepsy (ILAE).dd https://www.epilepsydiagnosis.org/.
[5] D.Y. Ko, S.R. Benbadis, Epilepsy and Seizures, Medscape, 2016.
[6] A. Krumholz, S. Wiebe, G. Gronseth, S. Shinnar, P. Levisohn, T. Ting, J. Hopp, P. Shafer, H. Morris, L. Seiden, G. Barkley, J. French, Quality standards subcommittee of the american academy of neurology, Practice Parameter: evaluating an apparent unprovoked first seizure in adults (an evidence-based review): report of the Quality Standards Subcommittee of the American Academy of Neurology and the American Epilepsy Society, American Epilepsy Society, Neurology 69 (21) (2007).
[7] H. Adeli, Z. Zhou, N. Dadmehr, Analysis of EEG records in an epileptic patient using wavelet transform, J. Neurosci. Meth. 123 (1) (2003) 69–87.
[8] U.R. Acharya, S.V. Sree, G. Swapna, R.J. Martis, J.S. Suri, Automated EEG analysis of epilepsy: a review, Knowl. Base Syst. 45 (2013) 147–165.
[9] O. Faust, U.R. Acharya, H. Adeli, A. Adeli, Wavelet-based EEG processing for computer-aided seizure detection and epilepsy diagnosis, Seizure 26 (2015) 56–64.
[10] U.R. Acharya, H. Fujita, V.K. Sudarshan, S. Bhat, J.E.W. Koh, Application of entropies for automated diagnosis of epilepsy using EEG signals: a review, Knowl. Base Syst. 88 (2015) 85–96.
[11] Y. LeCun, Y. Bengio, G. Hinton, Deep learning, Nature 521 (2015) 436–444.
[12] A. Krizhevsky, I. Sutskever, G.E. Hinton, ImageNet classification with deep convolutional neural networks, in: Neural Information Processing Systems Conference, 2012, 25.
[13] A. Ortiz-Garcia, J. Munilla, J.M. Gorriz, J. Ramirez, Ensembles of deep learning architectures for the early diagnosis of alzheimer's disease, Int. J. Neural Syst. 26 (2016) 7 (23 template pages).
[14] M.H. Rafiei, H. Adeli, A novel machine learning model for estimation of sale prices of real estate units, Construct. Eng. Manag. 142 (2) (2016) 04015066, https://doi.org/10.1061/(ASCE)Co.1943-7862.000104 (10 pages).
[15] M.H. Rafiei, W.H. Khushefati, R. Demirboga, H. Adeli, Supervised deep restricted boltzmann machine for estimation of concrete compressive strength, ACI Mater. J. 114 (2) (2017) 237–244.
[16] X. Glorot, A. Bordes, Y. Bengio, Deep sparse rectifier neural networks, J. Mach. Learn. Res. 15 (2010).
[17] I. Goodfellow, Y. Bengio, A. Courville, Deep Learning, MIT Press, 2016. http://www.deeplearningbook.org.
[18] J.G. Lee, S.H. Jun, Y.W. Cho, H. Lee, G.B. Kim, J.B. Seo, N. Kim, Deep learning in medical imaging: general overview, Korean J. Radiol. 18 (4) (2017) 570–584.
[19] R.G. Andrzejak, K. Lehnertz, C. Rieke, F. Mormann, P. David, C.E. Elger, Indications of nonlinear deterministic and finite dimensional structures in time series of brain electrical activity: dependence on recording region and brain state, Phys. Rev. E 64 (2001) 061907.
[20] N. Siddique, H. Adeli, Computational Intelligence - Synergies of Fuzzy Logic, Neural Networks and Evolutionary Computing, Wiley, West Sussex, United Kingdom, 2013 (512 pages).
[21] K. Fukushima, Neocognitron: a self-organizing neural network model for a mechanism of pattern recognition unaffected by shift in position, Biol. Cybern. 36 (1980) 193–202.
[22] M. Kallenberg, K. Petersen, M. Nielsen, Y.A. Ng, P.F. Diao, C. Igel, C.M. Vachon, K. Holland, R.R. Winkel, N. Karssemeijer, M. Lillholm, Unsupervised deep learning applied to breast density segmentation and mammographic risk scoring, IEEE Trans. Med. Imag. 35 (5) (2016) 1322–1331.
[23] S. Pereira, A. Pinto, V. Alves, C.A. Silva, Brain tumor segmentation using convolutional neural networks in MRI images, IEEE Trans. Med. Imag. 35 (5) (2016) 1240–1251.
[24] N. Hatipoglu, G. Bilgin, Cell segmentation in histopathological images with deep learning algorithms by utilizing spatial relationships, Med. Biol. Eng. Comput. (2017) 1–20, https://doi.org/10.1007/s11517-017-1630-1.
[25] J.H. Tan, U.R. Acharya, S.V. Bhandary, K.C. Chua, S. Sivaprasad, Segmentation of optic disc, fovea, and retinal vasculature using a single convolutional neural network, J. Comput. Sci. (2017), https://doi.org/10.1016/j.jocs.2017.02.006.
[26] A.A.A. Setio, F. Ciompi, G. Litjens, P. Gerke, C. Jacobs, S.J. van Riel, M.M.W. Wille, M. Naqibullah, C.I. Sánchex, B. van Ginneken, Pulmonary nodule detection in CT images: false positive reduction using multi-view convolutional networks, IEEE Trans. Med. Imag. 35 (5) (2016) 1160–1169.
[27] U.R. Acharya, H. Fujita, S.L. Oh, Y. Hagiwara, J.H. Tan, A. Muhammad, Application of deep convolutional neural network for automated detection of myocardial infarction using ECG signals, Inf. Sci. 415–416 (2017) 190–198.
[28] U.R. Acharya, H. Fujita, S.L. Oh, Y. Hagiwara, J.H. Tan, A. Muhammad, Automated detection of arrhythmias using different intervals of tachycardia ECG segments with convolutional neural network, Inf. Sci. 405 (2017) 81–90.
[29] U.R. Acharya, H. Fujita, S.L. Oh, A. Muhammad, J.H. Tan, K.C. Chua, Automated detection of coronary artery disease using different durations of ECG segments with convolutional neural network, Knowl. Base. Syst. (2017), https://doi.org/10.1016/j.knosys.2017.06.003.
[30] U.R. Acharya, S.L. Oh, Y. Hagiwara, J.H. Tan, M. Adam, A. Gertych, R.S. Tan, A deep convolutional neural network model to classify heartbeats, Comput. Biol. Med. (2017), https://doi.org/10.1016/j.compbiomed.2017.08.022.
[31] K. He, X. Zhang, S. Ren, J. Sun, Delving Deep into Rectifiers: Surpassing Human-level Performance on Image Net Classification, 2015, pp. 1026–1034.
[32] S.L. Hung, H. Adeli, Parallel backpropagation learning algorithms on cray Y-MP8/864 supercomputer, Neurocomputing 5 (6) (1993) 287–302.
[33] R.O. Duda, P.E. Hart, D.G. Stork, Pattern Classification 2nd Edition, John Wiley and Sons, New York, 2001.
[34] H. Adeli, S. Ghosh-Dastidar, N. Dadmehr, A wavelet-chaos methodology for analysis of EEGs and EEG sub-bands to detect seizure and epilepsy, IEEE Trans. Biomed. Eng. 54 (2) (2007) 205–211.
[35] W.Y. Hsu, Assembling a multi-feature EEG classifier for left-right motor data using wavelet-based fuzzy approximate entropy for improved accuracy, Int. J. Neural Syst. 25 (8) (2015) 1550037 (13 pages).
[36] Y. Yang, T. Solis-Escalante, J. Yao, A. Daffertshofer, A.C. Schouten, F.C.T. Van der Helm, A general approach for quantifying nonlinear connectivity in the nervous system based on phase coupling, Int. J. Neural Syst. 26 (1) (2016) 1550031 (19 pages).
[37] S. Ghosh-Dastidar, H. Adeli, N. Dadmehr, Mixed-band wavelet-chaos-neural network methodology for epilepsy and epileptic seizure detection, IEEE Trans. Biomed. Eng. 54 (9) (2007) 1545–1551.
[38] S. Ghosh-Dastidar, H. Adeli, N. Dadmehr, Principal component analysis-enhanced cosine radial basis function neural network for robust epilepsy and seizure detection, IEEE Trans. Biomed. Eng. 55 (2) (2008) 512–518.
[39] H. Adeli, S. Ghosh-Dastidar, Automated EEG-based Diagnosis of Neurological Disorders - Inventing the Future of Neurology, CRC Press, Taylor & Francis, Boca Raton, Florida, 2010.
[40] J.A. Garrido, N.R. Luque, S. Tolu, E. D'Angelo, Oscillation-driven spike-timing dependent plasticity allows multiple overlapping pattern recognition in inhibitory interneuron networks, Int. J. Neural Syst. 26 (2016) 5 (27 pages).
[41] S. Ghosh-Dastidar, H. Adeli, A new supervised learning algorithm for multiple spiking neural networks with application in epilepsy and seizure detection, Neural Netw. 22 (2009b) 1419–1431.
[42] S. Nobukawa, H. Nishimura, Enhancement of spike-timing dependent plasticity in spiking neural systems with noise, Int. J. Neural Syst. 26 (2016) 5 (11 pages).
[43] S. Ghosh-Dastidar, H. Adeli, Improved spiking neural networks for EEG classification and epilepsy and seizure detection, Integr. Computer-Aided Eng. 14 (3) (2007) 187–212.
[44] U.R. Acharya, K.C. Chua, T.C. Lim, Dorithy, J.S. Suri, Automatic identification of epileptic EEG signals using nonlinear parameters, J. Mech. Med. Biol. 9 (4) (2009) 539–553.
[45] U.R. Acharya, F. Molinari, S.V. Sree, S. Chattopadhay, K.H. Ng, Automated diagnosis of epileptic EEG using entropies, Biomed. Signal Process. Control 7 (4) (2012b), 410–408.
[46] U.R. Acharya, S.V. Sree, P.C.A. Ang, R. Yanti, J.S. Suri, Application of non-linear and wavelet based features for the automated identification of epileptic EEG signals, Int. J. Neural Syst. 22 (2) (2012a) 1250002-1–1250002-14.
[47] U.R. Acharya, S.V. Sree, S. Chattopadhyay, W.W. Yu, P.C.A. Ang, Application of recurrence quantification analysis for the automated identification of epileptic EEG signals, Int. J. Neural Syst. 21 (3) (2011a) 199–211.
[48] U.R. Acharya, S.V. Sree, P.C.A. Ang, J.S. Suri, Use of principal component analysis for automatic detection of epileptic EEG activities, Expert Syst. Appl. 39 (10) (2012c) 9072–9078.
[49] U.R. Acharya, S.V. Sree, J.S. Suri, Automatic detection of epileptic EEG signals using higher order cumulants features, Int. J. Neural Syst. 21 (5) (2011b) 403–414.
[50] U.R. Acharya, R. Yanti, G. Swapna, V.S. Sree, R.J. Martis, J.S. Suri, Automated diagnosis of epileptic electroencephalogram using independent component analysis and discrete wavelet transform for different electroencephalogram durations, Proceedings of the Institution of Mechanical Engineers. Part H, J. Eng. Med. 227 (3) (2012d).

[51] K.C. Chua, V. Chandran, U.R. Acharya, C.M. Lim, Automatic identification of epileptic electroencephalography signals using higher-order spectra, Proceedings of the Institution of Mechanical Engineers. Part H, J. Eng. Med. 223 (4) (2009) 485–495.

[52] K.C. Chua, V. Chandran, U.R. Acharya, C.M. Lim, Application of higher order spectra to identify epileptic EEG, J. Med. Syst. 35 (6) (2010) 1563–1571.

[53] O. Faust, U.R. Acharya, C.M. Lim, B.H. Sputh, Automatic identification of epileptic and background EEG signals using frequency domain parameters, Int. J. Neural Syst. 20 (2) (2010) 159–176.

[54] E. Castillo, D. Peteiro-Barral, B. Guijarro Berdinas, O. Fontenla-Romero, Distributed one-class support vector machine, Int. J. Neural Syst. 25 (7) (2015) 1550029 (17 pages).

[55] L. Guo, D. Rivero, J. Dorado, C.R. Munteanu, A. Pazos, Automatic feature extraction using genetic programming: an application to epileptic EEG classification, Expert Syst. Appl. 38 (2011) 10425–10436.

[56] Y. Zhang, W. Zhou, Multifractal analysis and relevance vector machine-based automatic seizure detection in intracranial EEG, Int. J. Neural Syst. 25 (6) (2015) 1550020 (14 pages).

[57] Z. Vahabi, R. Amirfattahi, F. Ghassemi, F. Shayegh, Online epileptic seizure prediction using wavelet-based bi-phase correlation of electrical signal tomography, Int. J. Neural Syst. 25 (6) (2015) 1550028 (22 pages).

[58] S. Yuan, W. Zhou, Q. Wu, Y. Zhang, Epileptic seizure detection with log-euclidean gaussian kernel-based sparse representation, Int. J. Neural Syst. 26 (3) (2016) 1650011 (15 pages).

[59] R.J. Martis, U.R. Acharya, J.H. Tan, A. Petznick, R. Yanti, K.C. Chua, E.Y.K. Ng, L. Tong, Application of empirical mode decomposition (EMD) for automated detection of epilepsy using EEG signals, Int. J. Neural Syst. 22 (6) (2012) 1250027-1–1250027-16.

[60] S. Ghosh-Dastidar, H. Adeli, Spiking neural networks, Int. J. Neural Syst. 19 (4) (2009a) 295–308.

[61] A. Bhattacharyya, R.B. Pachori, A multivariate approach for patient-specific EEG seizure detection using empirical wavelet transform, IEEE Trans. Biomed. Eng. 64 (9) (2017a) 2003–2015.

[62] A. Bhattacharyya, R.B. Pachori, A. Upadhyay, U.R. Acharya, Tunable-Q wavelet transform based multiscale entropy measure for automated classification of epileptic EEG signals, Appl. Signal Process. Meth. Syst. Anal. Physiol. Health 7 (4) (2017b) 385.

[63] M. Sharma, R.B. Pachori, U.R. Acharya, A new approach to characterize epileptic seizures using analytic time-frequency flexible wavelet transform and fractal dimension, Pattern Recognit. Lett. 94 (2017) 172–179.